Am J Physiol Lung Cell Mol Physiol 289: L698–L708, 2005.
First published June 10, 2005; doi:10.1152/ajplung.00084.2005.

Unusual inflammatory and fibrogenic pulmonary responses to single-walled carbon nanotubes in mice

Anna A. Shvedova,[1] Elena R. Kisin,[1] Robert Mercer,[1] Ashley R. Murray,[1] Victor J. Johnson,[1] Alla I. Potapovich,[4,5] Yulia Y. Tyurina,[4,5] Olga Gorelik,[3] Sevaram Arepalli,[3] Diane Schwegler-Berry,[1] Ann F. Hubbs,[1] James Antonini,[1] Douglas E. Evans,[2] Bon-Ki Ku,[2] Dawn Ramsey,[2] Andrew Maynard,[2] Valerian E. Kagan,[4,5] Vincent Castranova,[1,5] and Paul Baron[2]

[1]*Health Effects Laboratory Division, National Institute for Occupational Safety and Health, Morgantown, West Virginia;* [2]*Division of Applied Research and Technology, National Institute for Occupational Safety and Health, Cincinnati, Ohio;* [3]*Nanotube Team, GBTech, Incorporated, National Aeronautics and Space Administration-Johnson Space Center, Houston, Texas; and* [4]*Center for Free Radical & Antioxidant Health and* [5]*Department of Environmental Health, University of Pittsburgh, Pittsburgh, Pennsylvania*

Submitted 22 February 2005; accepted in final form 7 June 2005

Shvedova, Anna A., Elena R. Kisin, Robert Mercer, Ashley R. Murray, Victor J. Johnson, Alla I. Potapovich, Yulia Y. Tyurina, Olga Gorelik, Sevaram Arepalli, Diane Schwegler-Berry, Ann F. Hubbs, James Antonini, Douglas E. Evans, Bon-Ki Ku, Dawn Ramsey, Andrew Maynard, Valerian E. Kagan, Vincent Castranova, and Paul Baron. Unusual inflammatory and fibrogenic pulmonary responses to single-walled carbon nanotubes in mice. *Am J Physiol Lung Cell Mol Physiol* 289: L698–L708, 2005. First published June 10, 2005; doi:10.1152/ajplung.00084.2005.—Single-walled carbon nanotubes (SWCNT) are new materials of emerging technological importance. As SWCNT are introduced into the life cycle of commercial products, their effects on human health and environment should be addressed. We demonstrated that pharyngeal aspiration of SWCNT elicited unusual pulmonary effects in C57BL/6 mice that combined a robust but acute inflammation with early onset yet progressive fibrosis and granulomas. A dose-dependent increase in the protein, LDH, and γ-glutamyl transferase activities in bronchoalveolar lavage were found along with accumulation of 4-hydroxynonenal (oxidative biomarker) and depletion of glutathione in lungs. An early neutrophils accumulation (*day 1*), followed by lymphocyte (*day 3*) and macrophage (*day 7*) influx, was accompanied by early elevation of proinflammatory cytokines (TNF-α, IL-1β; *day 1*) followed by fibrogenic transforming growth factor (TGF)-β1 (peaked on *day 7*). A rapid progressive fibrosis found in mice exhibited two distinct morphologies: *1*) SWCNT-induced granulomas mainly associated with hypertrophied epithelial cells surrounding SWCNT aggregates and *2*) diffuse interstitial fibrosis and alveolar wall thickening likely associated with dispersed SWCNT. In vitro exposure of murine RAW 264.7 macrophages to SWCNT triggered TGF-β1 production similarly to zymosan but generated less TNF-α and IL-1β. SWCNT did not cause superoxide or NO· production, active SWCNT engulfment, or apoptosis in RAW 264.7 macrophages. Functional respiratory deficiencies and decreased bacterial clearance (*Listeria monocytogenes*) were found in mice treated with SWCNT. Equal doses of ultrafine carbon black particles or fine crystalline silica (SiO_2) did not induce granulomas or alveolar wall thickening and caused a significantly weaker pulmonary inflammation and damage.

nanoparticles; inflammation; cytokines; microbial infection

AS NANOMATERIALS and nanodevices are developed (22), awareness is growing that their unusual physicochemical properties may lead to new dilemmas in decision making and managing potential environmental and health risks (8, 9, 14, 16, 29). The UK government commissioned the Royal Society and the Royal Academy of Engineering to carry out a study into developments and impacts of nanotechnologies. The resulting report recognized that ". . .their application may raise new challenges in the safety, regulatory or ethical domains that will require societal debate" (23). The report placed particular emphasis on the potential impact of exposure to nanoparticles. At the time of this writing, only four reports have been published to document pulmonary toxicity of single-walled carbon nanotubes (SWCNT) or fullerenes (1, 14, 16, 29). In a very recent study, Warheit et al. (29) exposed rats by intratracheal instillation to SWCNT obtained by a laser ablation technology and reported transient inflammatory and cell injury effects as well as formation of multifocal granulomas centered around SWCNT aggregates. The toxicological relevance of these observations was judged questionable by the authors due to lack of a dose response, whereas the formation of granulomas was ascribed as the nonspecific outcome of given a bolus of agglomerated nanorope shaped SWCNT (29). In another study, Lam et al. (16) observed that a single intratracheal exposure of mice to SWCNT induced persistent epithelioid granulomas and interstitial inflammation. These pulmonary lesions in response to SWCNT were dose related, and the authors concluded that SWCNT were toxic. In light of these two studies, the pulmonary toxicity of SWCNT is currently a subject of debate. An objective of the present study is to resolve this conflict by a complete evaluation of the dose dependence and time course of pulmonary responses of mice to pharyngeal aspiration of SWCNT, which had been purified to remove contaminating metals.

Particle-induced pulmonary fibrosis has been associated with sustained inflammation, oxidative stress, and mediator release (20, 27). Our study was designed to assess various markers of inflammatory and fibrogenic pulmonary responses as well as oxidative stress response to SWCNT. Such a comprehensive characterization of SWCNT effects has not been performed in any of the earlier studies and should represent a first step in elucidating the mechanism(s) involved in the inflammatory response to SWCNT. To further evaluate mech-

Address for reprint requests and other correspondence: A. A. Shvedova, Health Effects Laboratory Div., NIOSH, Morgantown, WV (e-mail: AShvedova@cdc.gov).

The costs of publication of this article were defrayed in part by the payment of page charges. The article must therefore be hereby marked "*advertisement*" in accordance with 18 U.S.C. Section 1734 solely to indicate this fact.

anisms, we performed in vitro experiments to study the effects of SWCNT on RAW 264.7 macrophages. Parameters evaluated in this study included cytokine production, stimulation of reactive oxidant species, and particle uptake. The present study also conducted morphological investigation into the deposition and fate of aspirated SWCNT in the lung. Preliminary evidence is presented that SWCNT can penetrate to the interstitial tissue. Such penetration raises the possibility of further translocation into systemic circulation as has been earlier documented for other ultrafine particles (10, 19). Although not addressed in this study, systemic translocation is a topic of concern that requires investigation.

MATERIALS AND METHODS

Animals. Specific-pathogen-free adult female C57BL/6 mice (7–8 wk) were supplied by Jackson Lab (Bar Harbor, ME) and weighed 20.3 + 0.21 g at time of use. Animals were individually housed in American Association for Accreditation of Laboratory Animal Care-approved National Institute of Occupational Safety and Health (NIOSH) animal facilities in microisolator cages for 1 wk before use. Autoclaved Beta Chip bedding (Northeastern Products, Warrensburg, NY) was changed weekly. Animals were supplied with water and food (Harlan Teklad, 7913, NIH-31 Modified Mouse/Rat Diet, Irradiated; Harlan Teklad, Madison, WI) and housed under controlled light, temperature, and humidity conditions. Experiments were conducted under a protocol approved by the Animal Care and Use Committee of NIOSH.

General experimental design. To assess pulmonary toxicity of SWCNT, we randomized mice into six experimental groups treated with either SWCNT (0, 10, 20, 40 μg/mouse) or two reference materials [ultrafine carbon black (UfCB) or SiO_2, 40 μg/mouse] on *day 0*. Animals were killed 1, 3, 7, 28, and 60 days following exposures. Inflammation was evaluated by total cell counts, cell differentials, and accumulation of inflammatory cytokines [TNF-α, IL-1β, transforming growth factor (TGF)-β1] in the bronchoalveolar lavage (BAL) fluid. Pulmonary toxicity was assessed by elevation of lactate dehydrogenase (LDH) and γ-glutamyl transferase (GGT) activities, and protein levels in acellular BAL fluid. Fibrogenic responses to exposed materials were assessed by histopathological evaluation of fibrous collagen in lung tissues and by morphometric measurement of alveolar wall thickening. Accumulation/reduction of biomarkers of oxidative stress [4-hydroxy-2-nonenal (4-HNE) and glutathione (GSH)] was determined in BAL fluid and lung tissue. Functional respiratory deficiency after SWCNT exposure was assessed by measurement of pulmonary function and by decreased bacterial clearance (*Listeria monocytogenes*) in lung of inoculated mice. To assess in vitro cellular responsiveness to particles, murine RAW 264.7 macrophages were treated with SWCNT (0.1 mg/ml, 2–24 h, at 37°C). After SWCNT exposure, measurements of particle uptake, cytokine production, apoptotic cell accumulation, caspase-3/7 activity, generation of superoxide radicals [dihydroethidium (DHE) response], and generation of nitric oxide (NO·) [4,5-diaminofluorescein (DAF2) response] in macrophages were conducted.

Particles. SWCNT (CNI, Houston, TX) produced by the high-pressure CO disproportionation process (HiPco) technique (24), employing CO in a continuous-flow gas phase as the carbon feedstock and $Fe(CO)_5$ as the iron-containing catalyst precursor and purified by acid treatment to remove metal contaminates (12), were used in the study. Chemical analysis of total elemental carbon and trace metal (iron) in SWCNT was performed at the Chemical Exposure and Monitoring Branch (Division of Applied Research and Technology/NIOSH, Cincinnati, OH). Elemental carbon in SWCNT (HiPco) was assessed according to the NIOSH Manual of Analytical Methods (NMAN) (5), whereas metal content (iron) was analyzed by nitric acid dissolution and inductively coupled plasma-atomic emission spectrometry (ICP-AES). Analytical analysis performed by NMAN 5040 and ICP-AES revealed that SWCNT comprises 99.7% (wt) elemental carbon and 0.23% (wt) iron. For purity assessment of HiPco SWCNT, we used several standard analytical techniques, including thermogravimetric analysis with differential scanning colorimetry (TGA-DSC), thermo-programming oxidation (TPO), and Raman and near-infrared (NIR) spectroscopy (3, 4). Comparative analytical data obtained by TGA-DSC, TPO, NIR, and Raman spectroscopy revealed that >99% of carbon content in the SWCNT HiPco product was accountable in a carbon nanotube morphology. Purified suspended HiPco SWCNT (12) were used in the study (0.7 mg/ml). UfCB (Printex 90, Degussa, Germany) was a gift from Dr. G. Oberdorster (University of Rochester, Rochester, NY), crystalline silica (Min-U-Sil-5) was obtained from US Silica (Berkeley Springs, WV). The suspensions of carbon black and silica were prepared by sonification with phosphate-buffered saline (PBS) to disperse the particles with a Branson Sonifier 450 (Danbury, CT) for 2–3 min before animal exposure. The mean diameter and surface area of SWCNT, UfCB, or silica were 1–4 nm and 1,040 m^2/g, 14.3 nm and 254 m^2/g, or 2.14 μm and 4.95 m^2/g, respectively. Surface area was determined by Brunauer, Emmett, and Teller analysis, and diameter was measured by transmission electron microscopy (TEM).

Particulate instillation. Mouse pharyngeal aspiration was used for particulate administration. In brief, after anesthetization with a mixture of ketamine (Phoenix, St. Joseph, MO) and xylazine (Phoenix) (62.5 and 2.5 mg/kg subcutaneous in the abdominal area), the mouse was placed on a board in a near vertical position, and the animal's tongue was extended with lined forceps. A suspension (~50 μl) of particulates prepared in PBS (SWCNT at a dose of 0, 10, 20, 40 μg/mouse, UfCB, or SiO_2 at a dose of 40 μg/mouse) was placed posterior in the throat, and the tongue was held until the suspension was aspirated into the lungs. All particles were sterilized before administration. Control mice were administered sterile Ca^{2+} plus Mg^{2+}-free PBS vehicle. All mice in particle and PBS groups survived this exposure procedure. This technique provides good distribution of particles widely disseminated in a peribronchiolar pattern within the alveolar region (21). Animals treated with the particulates and PBS recovered easily after anesthesia with no behavioral or negative health outcomes. BAL cytology and cytokine assays from vehicle-control mice 1 day after exposure were used as a control to assure that pharyngeal aspiration did not translocate inflammatory material (such as bacteria) from the pharynx into the lung.

BAL. Mice were weighed and killed with intraperitoneal injection of pentobarbital sodium (>100 mg/kg; Fort Dodge Animal Health, Fort Dodge, IA). The trachea was cannulated with a blunted 22-gauge needle, and BAL was performed with cold sterile Ca^{2+} plus Mg^{2+}-free PBS at a volume of 0.9 ml for first lavage (kept separate) and 1.0 ml for subsequent lavages. Approximately 5 ml of BAL fluid per mouse were collected and pooled in sterile centrifuge tubes. Pooled BAL cells were washed in Ca^{2+} plus Mg^{2+}-free PBS by alternate centrifugation (800 *g* for 10 min at 4°C) and resuspension. Cell-free first-fraction BAL aliquots were frozen or kept until processed.

BAL cell counting and differentials. The degree of inflammatory response induced by the pharyngeal aspirated particulates was estimated by the total cells, macrophages, neutrophils, and lymphocytes recruited into the mouse lungs and recovered in the BAL fluid. Cell counts were performed with an electronic cell counter equipped with a cell sizing attachment (Coulter model Multisizer II with a 256C channelizer; Coulter Electronics, Hialeah, FL). Alveolar macrophages, polymorphonuclear leukocytes, and lymphocytes were identified by their characteristic cell shape in centrifuge smears stained with a Hema-3 kit (Fisher Scientific, Pittsburgh, PA), and differential counts of BAL cells were carried out. Three hundred cells per slide were counted.

Lung fixation and histopathology. Lung tissues were prepared for histological analysis under standard conditions. Animals were deeply anesthetized with an overdose of pentobarbital sodium. The trachea

was exposed, cannulated, and secured with a suture. Before instillation of fixative, the diaphragm was ruptured to collapse the lungs. The lungs were subsequently fixed with 1% paraformaldehyde-0.1% glutaraldehyde in situ at 5 cm of pressure for 0.2 h. Thereafter, the trachea was ligated, and the lungs were excised and submerged in fixative overnight before embedding. Lung tissue slices were prepared from both right and left lung lobes and embedded in paraffin. Sections (5 μm) were prepared with an HM 320 rotary microtome (Carl Zeiss, Thornwood, NY). Lung specimens were stained with hematoxylin and eosin or Masson's trichrome. Airways, terminal bronchioles, and the lung parenchyma were examined microscopically for the presence of cellular changes and inflammation.

Immunofluorescence technique. Paraffin-embedded sections of the left lung lobe were used for immunofluorescent detection of cytokeratin-8/18. After xylene deparaffinizating, cytokeratin-8/18 staining was done by the procedure described by Ghanem et al. (11). A polyclonal guinea pig anticytokeratin-8/18 was used as the primary antibody (Research Diagnostics, Flanders, NJ), and an FITC-labeled donkey anti-guinea pig IgG (Research Diagnostics) was used as the secondary antibody to detect cytokeratin. Slides were then visualized on an Olympus fluorescent photomicroscope (Olympus AX70; Olympus American, Lake Success, NY) with ×40 magnification using a green cube (460–500 nm excitation).

Sirius red staining. The distribution of fibrous collagen in lung tissue was determined by morphometric evaluation of specimens by Sirius red-polarizing microscopy. Sirius red F3BA was dissolved in saturated picric acid at a concentration of 1 g/l. Paraffin lung sections (5 μM thick) were deparaffinized and dehydrated with xylene-alcohol series to distilled water, immersed in alcohol-saturated picric acid for 20 min, and then washed with tap water until the yellow stain was cleared from the slides. To identify collagen fibers in light microscopy sections, the sections were stained with F3BA/picric acid for 1–2 h, washed with 0.01 N HCl for 1 min, and counterstained with Mayer's hematoxylin for 2 min. The slides were than dehydrated and mounted with coverslips (15). Quantitative morphometric methods were used to measure the average thickness of Sirius red-positive connective tissues in the alveolar wall and the Sirius red-positive connective tissues and cells in foci of granulomatous inflammation. Volume and surface density were measured by standard morphometric analyses (28). This consisted of basic point and intercept counting. Volume density was determined from counting the number of points over the Sirius red-positive connective tissues in the alveolar regions and points over Sirius red-positive connective tissues and cells in the granulomatous regions. Surface density of the alveolar wall and granulomatous regions was determined from intercepts between a line overlay and the alveolar wall. These point and intercept counts were made using a 121-point/11-line overlay graticule (12.5 mm square with 100 divisions) at ×40 magnification taken at six locations equally spaced across each section (one section per animal). This process was repeated twice for each animal. Areas containing airways or blood vessels >25 mm in diameter were excluded from the analysis. Average thickness of the Sirius red-positive connective tissues of the alveolar wall, Sirius red-positive connective tissues of granulomatous regions, and cells of granulomatous regions were computed from two times the ratio of volume density of point to the surface density of the alveolar wall.

TEM. TEM of a nebulized SWCNT suspension was used to investigate possible SWCNT morphologies generated by pharyngeal aspiration. Dilutions of SWCNT suspension in water (1:1 and 1:10) were aerosolized by ultrasonic nebulization (Mystique ultrasonic nebulizer; Air Sep, Buffalo, NY) and micro-pump nebulization (Aeroneb micro-pump nebulizer; Aerogen, Mountain View, CA). Each nebulizer had a manufacturer-reported mass median particle diameter of ~5 μm. Aerosols were generated into the top of ~10-l-volume cylindrical chamber and sampled onto an upward-facing 0.4-μm-pore Nucleopore filter supporting a 3-mm TEM grid coated with a lacey carbon. Aerosol samples were dried before being prepared for electron microscopy analysis. Analyses were carried out with a Philips EM420 TEM.

For electron microscope analysis of pulmonary tissue or cultured macrophages, lungs or RAW 264.7 macrophages were fixed in Karnovsky's fixative (2.5% glutaraldehyde + 3% paraformaldehyde in 0.1 M sodium cacodylate, pH 7.4) and postfixed with osmium tetroxide. Tissues or cells were dehydrated in graded alcohol solutions and propylene oxide and embedded in LX-112 (Ladd, Williston, VT). Ultrathin sections were stained with uranyl acetate and lead citrate and examined with a TEM (JEOL 1220, Tokyo, Japan).

TGF-β1, TNF-α, IL-1β, and 4-HNE in BAL fluid and RAW 264.7 macrophage-conditioned medium. Measurements of TGF-β1, TNF-α, IL-1β, and 4-HNE were performed in the acellular BAL fluid on *days 1, 3, 7,* and *28* following SWCNT exposures. The concentrations of active TGF-β1, TNF-α, IL-1β, and 4-HNE (sensitivity of assay is 0.1 pg/ml) were determined by Super-ELISA (BioTraces, Herndon, VA) according to the proprietary protocol (see website: www.biotraces.com for more information) using commercially available antibodies (R&D Systems, Minneapolis, MN). Mediator release from RAW 264.7 macrophages treated with SWCNT (0.1 mg/ml) or zymosan (0.25 mg/ml) for 6 h was measured by Super-ELISA as described above.

Total protein, LDH activity, and GGT activity in BAL fluid. Measurement of total protein in the BAL supernatant was performed by a modified Bradford assay according to the manufacturer's instructions (Bio-Rad, Hercules, CA) with bovine serum albumin as a standard. We assayed the activity of LDH spectrophotometrically by monitoring the reduction of nicotinamide adenine dinucleotide at 340 nm in the presence of lactate (Pointe Scientific, Lincoln Park, MI). GGT activity was measured spectrophotometrically with the diagnostic kit (Pointe Scientific) adapted for use on a 96-well plate.

Fluorescence assay of GSH. GSH concentration in lung homogenates was determined with ThioGlo-1, a maleimide reagent that produces a highly fluorescent adduct upon its reaction with SH− groups (25). GSH content was estimated by an immediate fluorescence response registered upon addition of ThioGlo-1 to the lung homogenate. A standard curve was established by addition of GSH (0.04–4.0 μM) to 100 mM disodium phosphate buffer (pH 7.4) containing 10 μM ThioGlo-1 (DMSO solution). A spectrofluorophotometer RF-5301PC (Shimadzu, Kyoto, Japan) was employed for the assay of fluorescence using excitation at 388 nm and emission at 500 nm. The data obtained were exported and analyzed using RF-5301PC Personal Fluorescence software (Shimadzu).

Cell culture. RAW 264.7 macrophages (ATCC, Manassas, VA) were grown in DMEM supplemented with 10% heat-inactivated FBS, 100 units/ml penicillin, and 100 μg/ml streptomycin in a humidified atmosphere (5% CO_2 plus 95% air) at 37°C.

Assessment of apoptotic cells and caspase-3/7 activity in RAW 264.7 macrophages. RAW 264.7 macrophages (0.05×10^6/well) were incubated with SWCNT for 4–6 h at 37°C. Then cells were washed and fixed with 2% of paraformaldehyde. Nuclear condensation and fragmentation was assessed by Hoechst 33342 (Molecular Probes, Eugene, OR) staining (2 mg/ml, for 1 h for 4°C). The number of apoptotic macrophages was scored by fluorescence microscopy (Nikon, Eclipse TE200, 4′,6-diamidino-2-phenylindole filter). Caspase-3/7 activity in RAW 264.7 macrophages (1.0×10^6/well) stimulated by SWCNT or zymosan for 2, 6, 18, or 24 h at 37°C was determined with a luminescence Caspase-Glo 3/7 Assay Kit (Promega, Madison, WI) as described in the manufacturer's instructions.

Generation of superoxide (DHE response) and NO·(DAF2 response) by RAW 264.7 macrophages. DHE and 4,5-diaminofluorescein diacetate (DAF-2DA) were utilized to assess effects of SWCNT or zymosan on superoxide and NO· production, respectively. RAW 264.7 macrophages (0.3×10^6/well) were preincubated for 10 min at 37°C with 10 μM DHE (Molecular Probes) and incubated with SWCNT or zymosan (for 6 h at 37°C). Naïve or LPS-primed (0.1 μg/ml for 12 h at 37°C) RAW 264.7 macrophages were preincubated

for 1 h at 37°C with 2 μM DAF-2DA (Calbiochem, San Diego, CA) and coincubated with SWCNT or zymosan (for 2 h at 37°C). DHE- and DAF2-positive macrophages were assessed by flow cytometry (FACScan; Becton-Dickinson, San Jose, CA) by monitoring fluorescence (excitation 488 nm and emission 565–585 nm for channel FL-2, excitation 488 nm and emission 530 nm for channel FL-1, respectively). Ten thousand events were collected and analyzed with CellQuest software (Becton-Dickinson, San Jose, CA).

Measurement of pulmonary function. Spontaneous breathing patterns were monitored by whole body plethysmography. Breathing patterns were monitored 24 h before SWCNT exposure (baseline) and then 1, 3, 7, 28, and 60 days following exposure to detect treatment-related changes. Mice were acclimated to the plethysmograph for 10 min followed by 10 min of acquisition of spontaneous breathing data. Expiratory time was calculated from the raw waveforms with Biosystem XA software (Buxco Electronics, Wilmington, NC) and expressed as percentage of baseline.

Pulmonary bacterial inoculation and clearance. L. monocytogenes (strain 10403S, serotype 1) was cultured overnight in brain-heart infusion broth at 37°C in a shaking incubator. After incubation, the bacterial concentration was determined at an optical density of 600 nm and diluted with sterile saline to a concentration of 1×10^3 *L. monocytogenes* in 40 μl of sterile saline. At 3 days after treatment with SWCNT or saline, the mice were further divided and inoculated by pharyngeal aspiration with *L. monocytogenes* or sterile saline. In a previous pilot study, this bacterial dose did not elicit a significant inflammatory response in the lungs, gave a uniform infection, and did not have any effect on the mortality of untreated naïve C57BL/6 mice. At 1, 3, and 7 days post-*L. monocytogenes* inoculation, the lungs were removed from the mice from each treatment group. The excised lung tissues were suspended in 5 ml of sterile water, homogenized, and cultured on brain-heart infusion agar plates. The number of viable colony-forming units was counted after an overnight incubation at 37°C.

Statistical analysis. Results were compared by one-way ANOVA using the all pairwise multiple comparison procedures (Holm-Sidak method). All results are presented as means ± SE. P values of <0.05 were considered to be statistically significant.

RESULTS AND DISCUSSION

Among different types of nanoparticles, SWCNT with their unique electronic and mechanical properties may be also uniquely toxic to life, thus necessitating evaluation of their toxicity. As unintended occupational or environmental inhalation of SWCNT is not inconceivable, we studied the pulmonary responses of C57BL/6 mice to SWCNT delivery by pharyngeal aspiration. Occupationally relevant exposures were chosen based on the OSHA permissible exposure limit (PEL) for graphite particles: 5.0 mg/m^3, 8-h workday, 40 h/wk (18). The dose deposited in a person being exposed to the PEL for 20 8-h workdays would be equivalent to aspiration of a 20-μg SWCNT dose in the mouse. Therefore, for the pharyngeal aspiration exposures, we utilized the range of doses from 10 to 40 μg SWCNT per mouse.

To characterize the purified HiPco SWCNT used in this study (6), chemical analysis was performed by NMAN 5040 and IPC-AES and revealed that SWCNT comprises 99.7% (wt) elemental carbon and 0.23% (wt) of iron. Comparative analytical data obtained by TGA-DSC, TPO, NIR, and Raman spectroscopy revealed that >99% of carbon content in the SWCNT HiPco product was accountable in a carbon nanotube morphology. In line with this, analysis of purified SWCNT samples by electron paramagnetic resonance (EPR) spectroscopy revealed no signals from paramagnetic centers that are readily detectable in nonpurified samples as a broad signal with a g value of 2.0 and half-width of 640 G.

SWCNT suspension droplets that were dried and analyzed under a TEM did not show discrete agglomerates of carbon nanomaterial but exhibited a continuous mat of intertwined carbon nanoropes with varying diameters. It was reasoned that the physical characteristics of the material depositing in the lungs from such a suspension would be strongly influenced by the delivery mechanism. We therefore investigated the potential physical characteristics of the delivered SWCNT material further.

Under the hypothesis that the SWCNT delivery mechanism involved partial aerosolization of the suspension droplet during pharyngeal aspiration, fine droplets of the SWCNT suspension were generated by nebulization, and the resulting carbon nanotube particles were studied by TEM. Two distinct particle morphologies were observed: compact SWCNT aggregates (Fig. 1*A*) and dispersed SWCNT structures (Fig. 1*B*). Further investigation of dried suspension samples using the TEM and scanning electron microscope suggested that the compact aggregates may have been present as discrete particles within the suspension, but the data were not conclusive. Alternatively, it is feasible that the two morphologies observed were associated with suspension droplets drying before or after collection.

Accordingly, two morphologically distinct responses were detected in the lung as early as 7 days postexposure. Morphological response varied depending upon the association with dense SWCNT aggregates. Foci of granulomatous inflammation, including discrete granulomas often surrounded by hypertrophied epithelial cells, were associated with dense SWCNT aggregates (Fig. 1*D*). The carbon nanotube material was clearly visualized with granulomatous inflammation (Fig. 1, *E* and *F*), and interfacing bundles of fibrous connective tissue were observed within discrete granulomas. In lung regions distant from observed SWCNT aggregates, morphological alterations were predominantly diffuse interstitial fibrosis with alveolar wall thickening. Importantly, deposition of collagen and elastin was also observed in both granulomatous regions as well as in the areas distant from granulomas. This was established by conventional light microscopy of lung sections specifically stained with Sirius red (Fig. 1*D*) as well as by TEM (Fig. 1*H*). The fibrotic response progressed with time, with alveolar wall thickening being significantly greater at 60 days than 28 days postexposure (Fig. 1*G*, *inset*). Morphometric analysis indicated a significant granulomatous response, a significant fibrotic response within granulomas, and significant alveolar septal fibrosis (Fig. 1*G*). We observed that studied reference materials (UfCB and SiO_2), in contrast to SWCNT, *1*) did not cause thickening of alveolar walls, *2*) did not induce formation of granulomas, and *3*) resulted in a significantly lower magnitudes of inflammatory responses (cell differentials, cell counts, and protein in BAL) when animals were exposed to comparable doses of these particles (Fig. 2).

We further investigated whether the exposure caused significant damage to pulmonary cells. Increased numbers of alveolar type II (AT-II) cells, the progenitor cells that replicate following alveolar type I (AT-I) cell death, were noted in response to SWCNT. This was confirmed (Fig. 3*B*) by increased immunofluorescent detection of cytokeratins 8/18, markers of AT-II cells in the alveolus (11) and by increased

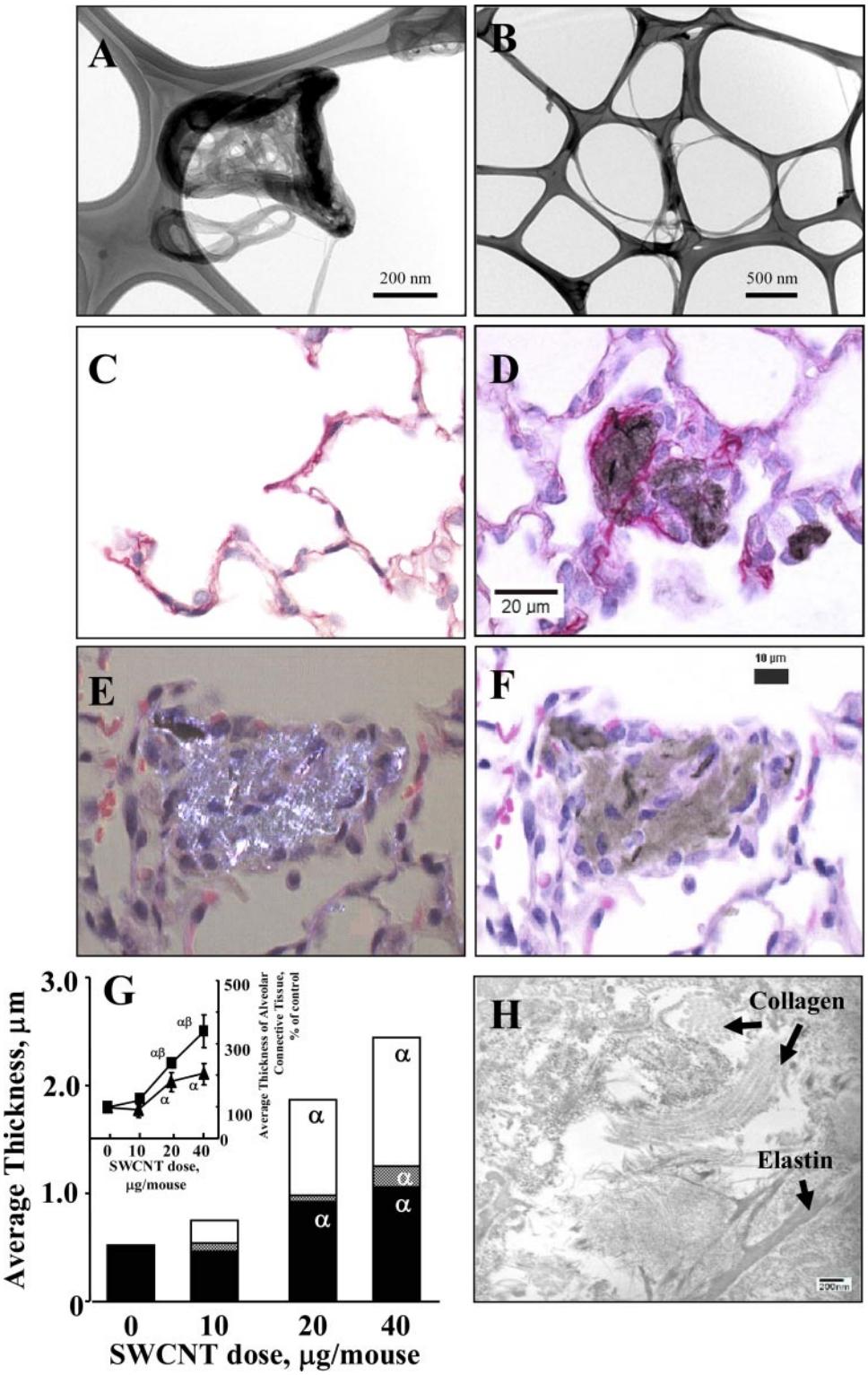

Fig. 1. *A*: transmission electron microscopy (TEM) image of a typical densely aggregated single-walled carbon nanotube (SWCNT) aerosol particle collected onto a lacey carbon support film. *B*: TEM image of a typical disperse structured SWCNT aerosol particle collected onto a lacey carbon support film. *C*: Sirius red-stained lung sections 7 days after aspiration of PBS (control mice). *D*: Sirius red-stained lung sections demonstrating focal granulomatous inflammation 7 days after aspiration of 40 μg SWCNT/mouse. *E*: polarized light photomicrograph demonstrating the presence of carbon nanotube material in a pulmonary granulomatous lesion 2 mo after aspiration. *F*: SWCNT are visualized as gray areas in the corresponding transmitted light section. *G*: morphometric measurement of connective and cellular tissues of lung sections in response to 10–40 μg/mouse SWCNT 28 days postpharyngeal aspiration (open bar, granulomatous cellular tissue; gray bar, granulomatous connective tissue; black bar, alveolar connective tissue). *Inset*: morphometric changes in connective tissue of alveolar wall regions in response to SWCNT (10–40 μg/mouse) 28 and 60 days posttreatment (▲, 28 days; ■, 60 days); means ± SE (n = 6 mice/group). $^{\alpha}P < 0.05$ vs. PBS-treated control mice; $^{\beta}P < 0.05$ vs. mice treated with 10 μg/mouse SWCNT. *H*: TEM of lung interstitium shows deposition of collagen and elastin.

numbers of cells expressing cytoplasmic lamellar bodies in TEM sections. This proliferation of AT-II cells indicates either AT-I cell injury, proliferation of AT-II cells to cover new basement membrane associated with the nodules, or both. To more accurately determine the level of cell injury, assays of protein content, LDH, and γ-glutamyl transferase (GGT) in the acellular BAL fluid obtained from the mice were performed. A dose-dependent and early (1–3 days postexposure) increase in the level of protein and LDH activity in acellular BAL fluid was observed (Fig. 4, *A* and *B*). Cell damage (LDH activity) was dose dependently increased 1 day postexposure and remained elevated until 28 days postexposure, whereas damage to the alveolar air-blood barrier, measured as increased protein secretion in BAL fluid, peaked at 3 days and declined there-

after. Activity of GGT was dose dependently increased with significant elevations observed 3 days postexposure and increases being sustained through 60 days (Fig. 4*C*). Exposure to SWCNT also resulted in the accumulation of a characteristic biomarker of oxidative stress, 4-HNE, in BAL fluid as early as 1 day postexposure (Fig. 4*D*). There also was a dose- and time-dependent depletion of a major antioxidant, GSH, in the lung being most severe 1 day postexposure (Fig. 4*E*).

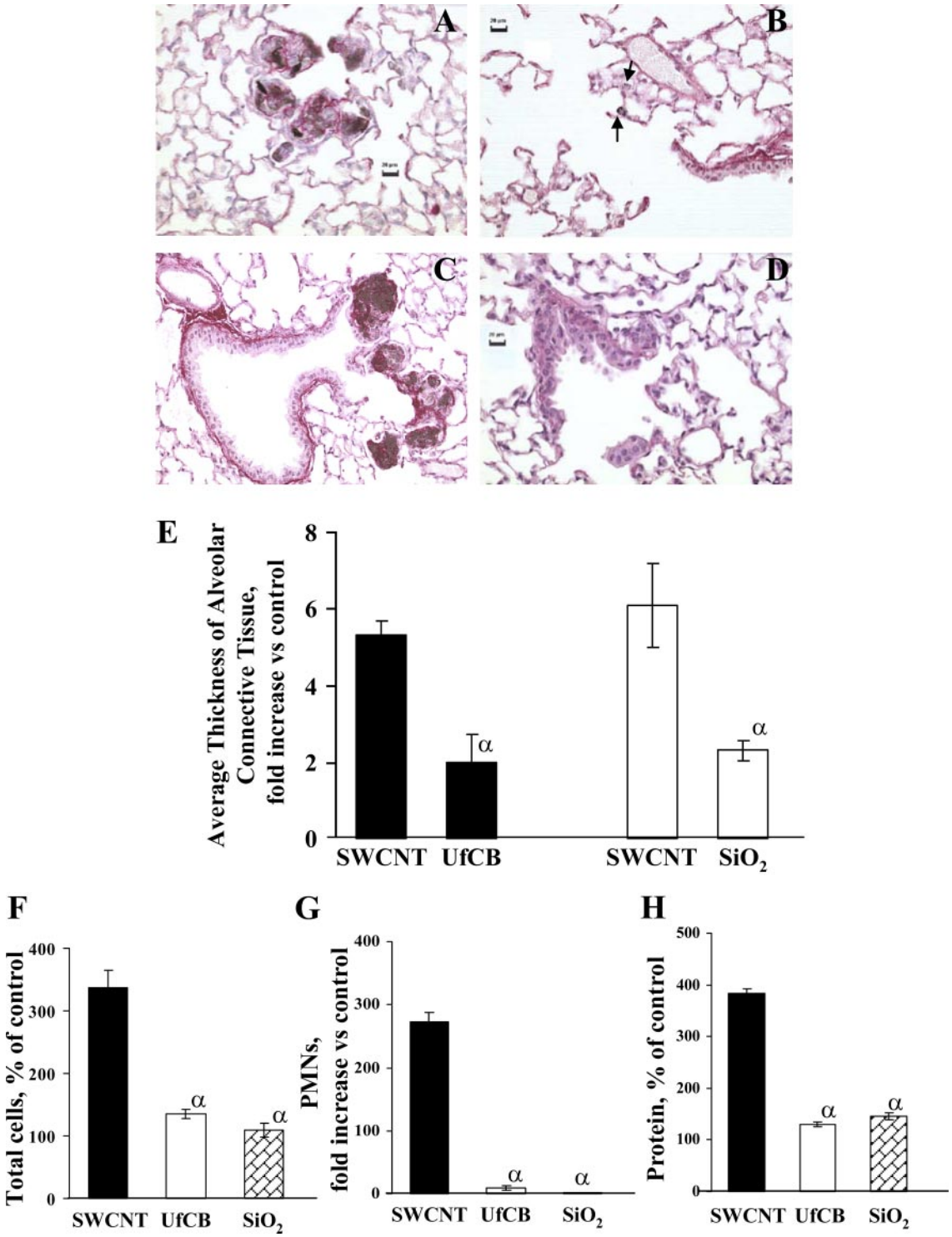

Fig. 2. Light micrographs of Sirius red-stained sections from lung of mice exposed to SWCNT, SiO_2, or ultrafine carbon black (UfCB, 40 μg/mouse). Sirius red-stained lung sections demonstrating effect of SWCNT (*A*) or UfCB (*B*) 28 days after aspiration. Arrows show residual carbon black particles present in individual macrophages. Sirius red-stained lung sections demonstrating effect of SWCNT (*C*) or SiO_2 (*D*) 60 days after aspiration. *E*: morphometric measurement of alveolar connective tissues of lung sections in response to 40 μg/mouse SWCNT, SiO_2, or UfCB 28 or 60 days posttreatment (solid bars, 28 days; open bars, 60 days); means ± SE ($n = 6$ mice/group). $^{\alpha}P < 0.05$ vs. SWCNT-treated mice. Inflammatory responses 24 h after aspiration of 40 μg/mouse SWCNT, UfCB, or SiO_2 evaluated by the changes in the total cell counts (*F*), polymorphonuclear neutrophils (PMNs, *G*), and protein (*H*) in the bronchoalveolar lavage (BAL) fluid of mice. $^{\alpha}P < 0.05$ vs. SWCNT-treated mice.

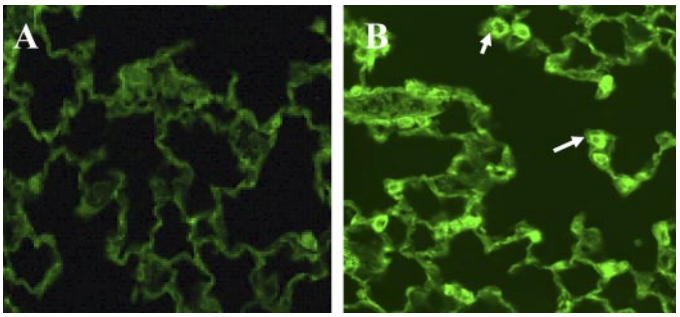

Fig. 3. Immunofluorescent staining of cytokeratins 8/18 expressed in alveolar type II (white arrows) of mouse alveoli 1 day after exposure to PBS (*A*) or 40 μg/mouse SWCNT (*B*); ×40 magnification.

BAL cytology indicated a robust and early (*day 1*) accumulation of neutrophils, followed by a sequential appearance of lymphocytes (peak 3 days) and macrophages (peak 7 days) (Fig. 5). These cellular responses increased with exposure dose. In line with these findings, proinflammatory cytokines (TNF-α, IL-1β) in the acellular BAL fluid were increased by 16- and 10-fold, respectively, on *day 1* and rapidly returned to near control levels at 3 days after exposure (Fig. 6, *A* and *B*). In contrast, fibrogenic TGF-β1 was not significantly increased until *day 7* and returned toward control by 28 days postexposure (Fig. 6*C*). Thus the time course of TNF-α and IL-1β corresponded to PMN influx, whereas that for TGF-β1 paralleled macrophage recruitment.

Assuming that macrophages may be significant contributors to the production of fibrogenic cytokines, we next investigated effects of SWCNT on murine RAW 264.7 macrophages in vitro. SWCNT were ultrasonicated to produce mainly nanoropes and more dispersed structures before being introduced to the cell cultures, as verified by TEM analysis. SWCNT were potent stimulants of TGF-β1 production, with effects similar to the classical stimulant, zymosan (Fig. 7*A*). In contrast, SWCNT produced markedly lower levels of TNF-α and IL-1β than that elicited by zymosan. SWCNT exposure of RAW 264.7 macrophages in vitro did not result in an oxidative burst or NO·production (Fig. 7, *B* and *C*). Moreover, RAW 264.7 macrophages did not appear to actively engulf SWCNT (Fig. 7*D*). In line with this, we did not observe any significant apoptosis of macrophages upon their incubation with SWCNT (Fig. 7*E*). Interestingly, a recent study using fluorescence NIR imaging microscopy (7) reported that macrophages can ingest detergent (Pluronic)-solubilized SWCNT without showing significant toxicity.

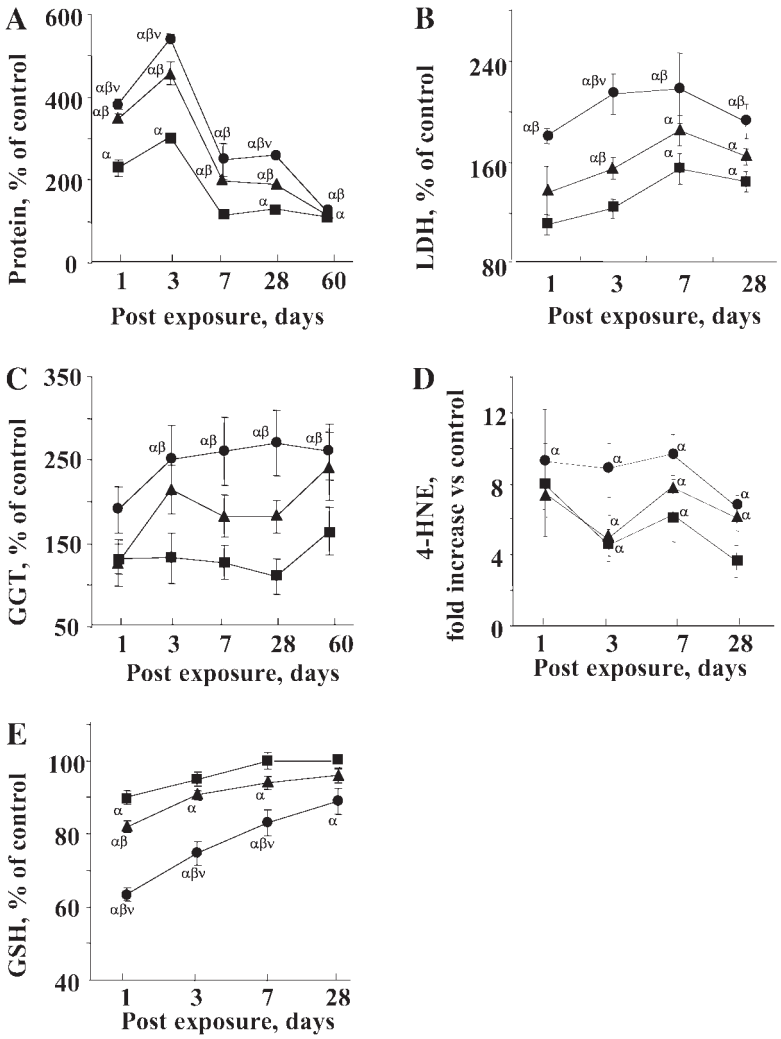

Fig. 4. Pulmonary cells damage following aspiration of 10–40 μg/mouse SWCNT evaluated by the changes in the level of protein (*A*), LDH activity (*B*), and GGT activity (*C*) in the BAL fluid of mice (■, 10 μg/mouse SWCNT; ▲, 20 μg/mouse SWCNT; ●, 40 μg/mouse SWCNT). Data are expressed as % of controls or fold increase vs. controls exposed to PBS. The degree of oxidative stress evaluated by 4-hydroxy-2-nonenal (4-HNE, *D*) in BAL fluid and GSH (*E*) in the lung of mice exposed to 10–40 μg/mouse SWCNT (■, 10 μg/mouse SWCNT; ▲, 20 μg/mouse SWCNT; ●, 40 μg/mouse SWCNT). Means ± SE (n = 12 mice/group). $^{\alpha}P <$ 0.05 vs. PBS-treated control mice; $^{\beta}P < 0.05$ vs. mice treated with 10 μg/mouse SWCNT; $^{\nu}P < 0.05$ vs. mice treated with 20 μg/mouse SWCNT.

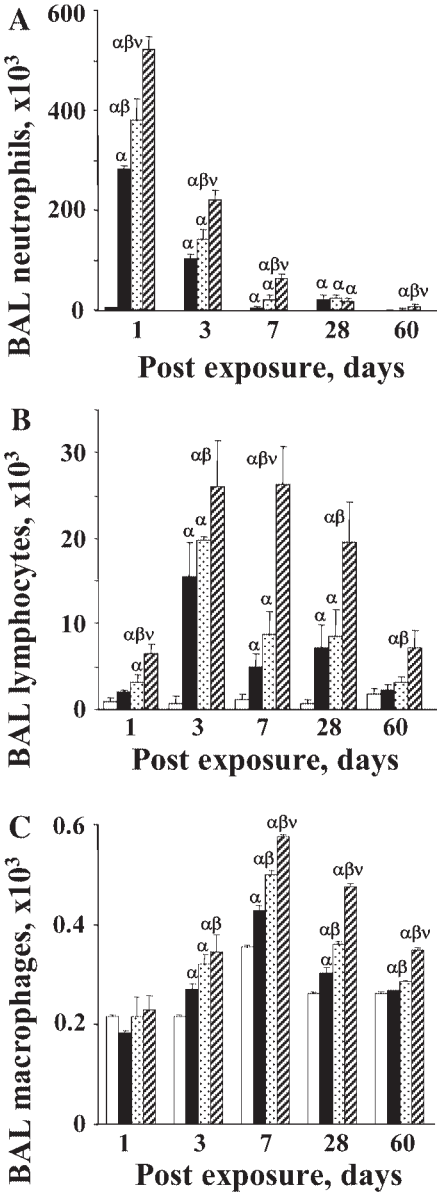

Fig. 5. Cell profile of BAL samples from mice after pharyngeal aspiration with SWCNT. *A*: PMNs; *B*: lymphocytes; *C*: macrophages (open bar, PBS; solid bar, 10 μg/mouse SWCNT; dotted bar, 20 μg/mouse SWCNT; hatched bar, 40 μg/mouse SWCNT). Means ± SE (n = 12 mice/group). $^{\alpha}P < 0.05$ vs. PBS-treated control mice; $^{\beta}P < 0.05$ vs. mice treated with 10 μg/mouse SWCNT; $^{\nu}P < 0.05$ vs. mice treated with 20 μg/mouse SWCNT.

Inflammation and fibrogenesis in the lung can lead to a detrimental decline in pulmonary function. Therefore, we determined whether SWCNT exposure caused altered pulmonary function. Importantly, a dose-dependent increase in expiratory time, a parameter shown to correlate with increased pulmonary resistance in the C57BL/6 mouse (2), was observed as early as *day 1* following SWCNT exposure and persisted for at least 60 days (Fig. 8*A*).

Because realistic exposures to SWCNT are likely to occur in conjunction with other pathogenic impacts, e.g., microbial infections, we tested whether combined exposures to SWCNT (*day 0*) and infectious agents (*L. monocytogenes, day 3*) could cause potentially synergistic responses. Bacterial clearance from the lungs of SWCNT (40 μg/mouse)-exposed mice was significantly slower compared with saline-treated controls 7 days after inoculation with bacteria (Fig. 8*B*).

Recent evidence suggests that chronic exposure to high levels of ambient particulate matter is associated with decreased pulmonary function, airway inflammation, and alterations in breathing patterns. It has been proposed that occupational exposure to ultrafine particles, such as carbon black, welding fumes, and diesel exhaust, may also be associated with pulmonary diseases. SWCNT are among newly developed products and are currently of interest for a variety of applications in electronics, reinforced rods, microfabricating conjugated polymer activators, supersensitive sensors, enhanced electron/scanning microscopy imaging techniques, and biosensors. Nanoengineered particles are already in consumer prod-

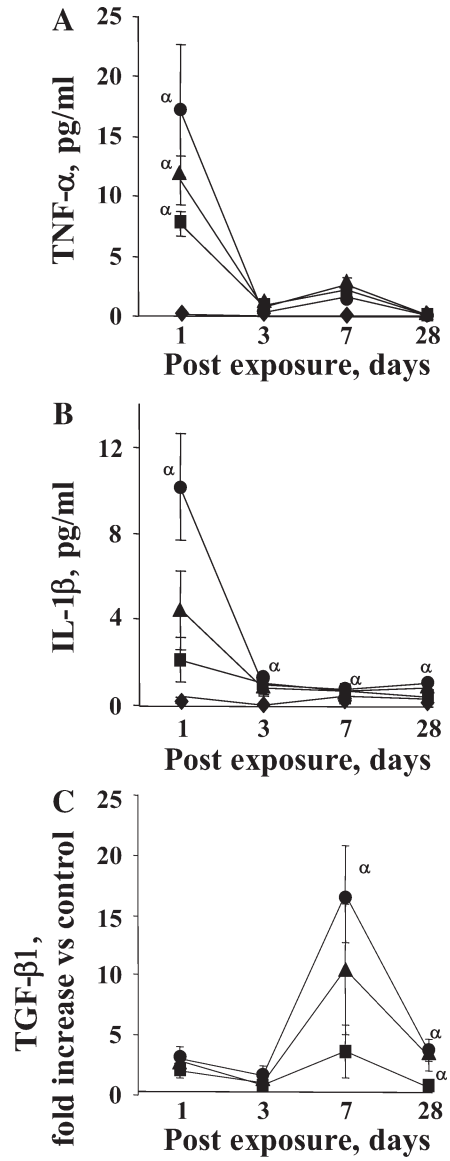

Fig. 6. Cytokine accumulation in the BAL fluid of mice following aspiration of 10–40 μg/mouse SWCNT evaluated by changes in the level of TNF-α (*A*), IL-1β (*B*), and transforming growth factor (TGF)-β1 (*C*). ◆, PBS; ■, 10 μg/mouse SWCNT; ▲, 20 μg/mouse SWCNT; ●, 40 μg/mouse SWCNT. Means ± SE (n = 12 mice/group). $^{\alpha}P < 0.05$ vs. PBS-treated control mice.

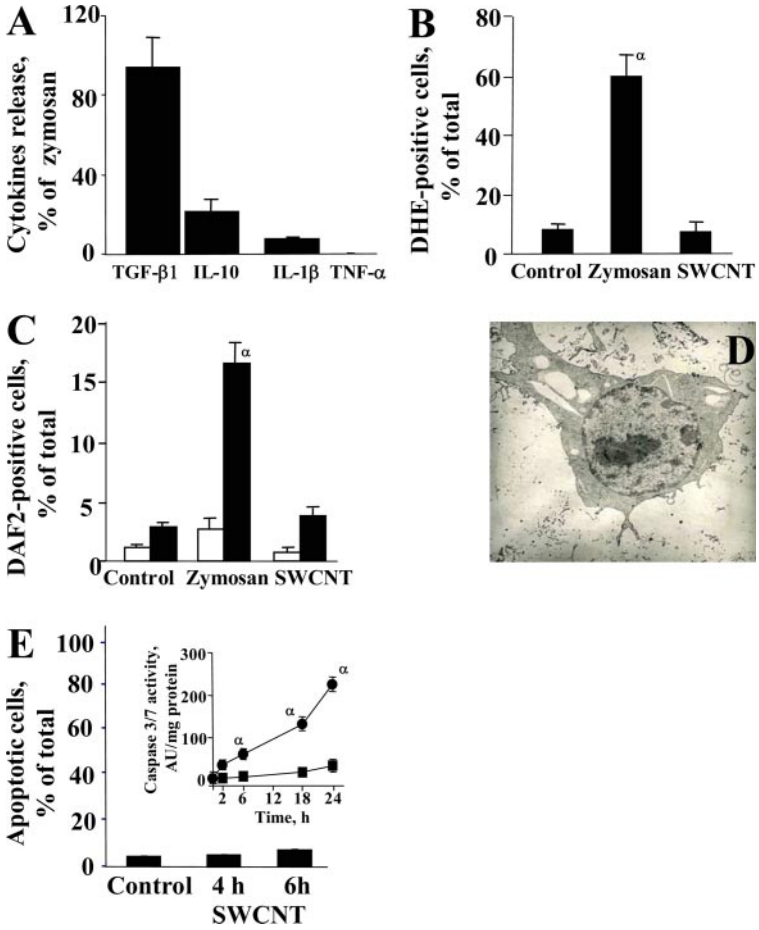

Fig. 7. RAW 264.7 macrophages were treated with SWCNT (0.1 mg/ml) or zymosan (0.25 mg/ml) and responses monitored. *A*: production of cytokines by RAW 264.7 macrophages incubated with SWCNT for 6 h. Data are expressed as % of zymosan-induced production. Generation of superoxide (*B*) and nitric oxide (NO·, *C*) by RAW 264.7 macrophages following incubation with SWCNT (0.1 mg/ml) or zymosan (0.25 mg/ml) for 6 or 2 h, respectively. DHE, dihydroethidium. *C*: for NO·production RAW 264.7 macrophages were not pretreated with LPS (open bar) or were pretreated with LPS (solid bar). Data are displayed as means ± SE for at least 9 experiments; $^{\alpha}P < 0.05$ vs. control cells. DAF2, 4,5-diaminofluorescein. *D*: electron micrograph of a RAW 264.7 macrophage incubated with SWCNT (0.1 mg/ml) for 6 h. Micrograph shown is representative of 3 independent experiments. Assessment of apoptotic cells (*E*) and caspase-3/7 activity (*inset*) in RAW 264.7 macrophages incubated in the presence of SWCNT or zymosan (■, 0.1 mg/ml SWCNT; ●, 0.25 mg/ml zymosan) for the times indicated. Data are displayed as means ± SE for at least 6 experiments; $^{\alpha}P < 0.05$ vs. cells incubated in the presence of SWCNT.

ucts, such as sunscreens, cosmetics, and toiletry goods, which are used daily by millions. The market for these materials is estimated to grow to over eight billion dollars in the next decade. Introduction of novel materials into industry requires evaluating safety and an understanding of the impact of nanomaterials on the environment, biological species, and human health.

The extremely small size (~1 nm in diameter) of SWCNT renders their chemical and physical properties fundamentally different from larger particles of the same composition. Therefore, the biological and toxicological effects of SWCNT cannot be predicted by extrapolation of data collected with fine carbon particles. The most commonly used technology in the manufacturing of SWCNT is catalytic disproportionation of gaseous carbon molecules supported on catalytic iron particles. SWCNT produced in the HiPco process usually contain significant amounts (up to 40% wt) of iron that may act as a catalyst of oxidative stress. Our lab has reported that such an unpurified SWCNT sample can generate reactive oxygen species and would produce oxidant stress and cytotoxicity in an in vitro bronchial epithelial cell model (25). The lung is the prime target for SWCNT toxicity as they can be inhaled during technological processing and use. Therefore, the pulmonary toxicity of SWCNT requires investigation. Lam et al. (16) and Warheit et al. (29) evaluated the pulmonary toxicity of unpurified SWCNT after intratracheal instillation in a mouse or rat model, respectively. Both studies reported an epithelial granulomatous reaction to SWCNT. Lam et al. (16) interpreted their results as indicating that SWCNT were toxic to the lung. However, Warheit et al. (29) failed to find a dose dependence of this granulomatous response and did not observe prolonged inflammation; therefore, they concluded that granulomas were a nonspecific response to instilled aggregates of SWCNT, which may not be relevant to human exposures. The objective of this present study was to resolve this conflict. In our study, purified SWCNT were used to avoid generation of oxidants from significant iron contamination. Indeed, the SWCNT sample used in the present study contained only 0.23% iron by weight and did not generate detectable signals from iron paramagnetic centers readily detectable by EPR spectroscopy in unpurified samples.

The present study also used pharyngeal aspiration as the exposure technique. As shown in Fig. 1, aspiration was likely to generate not only aggregates of SWCNT but more dispersed SWCNT structures. Results of the present study indicate the aspiration of SWCNT did cause an acute inflammatory reaction marked by a rapid increase in BAL levels of inflammatory cells, inflammatory cytokines, and protein. This acute inflammation resolved and did not persist over the 2-mo postexposure period. This transient inflammation correlated with the low reactivity of SWCNT to macrophages, inducing little particle uptake, cytokine production, superoxide generation, or NO production in vitro. As with studies by Lam et al. (16) and Warheit et al. (29), epitheloid granulomas were observed at deposition sites of SWCNT aggregates. This granuloma formation was rapid (within 7 days) and dose dependent and

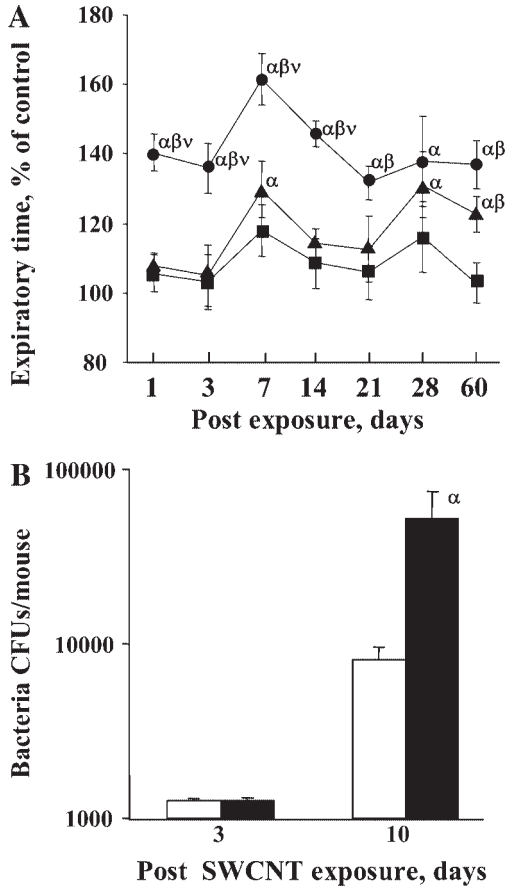

Fig. 8. *A*: a single aspiration of SWCNT leads to a rapid and persistent increase in expiratory time in C57BL/6 mice (■, 10 μg/mouse SWCNT; ▲, 20 μg/mouse SWCNT; ●, 40 μg/mouse SWCNT). Means ± SE (n = 6 mice/group). $^{\alpha}P < 0.05$ vs. PBS-treated control mice; $^{\beta}P < 0.05$ vs. mice treated with 10 μg/mouse SWCNT; $^{\nu}P < 0.05$ vs. mice treated with 20 μg/mouse SWCNT. *B*: assessment of pulmonary bacterial clearance in C57BL/6 mice after challenge with SWCNT (*day 0*) and *Listeria* (*day 3*) (open bar, PBS; solid bar, 40 μg/mouse SWCNT). CFU, colony-forming units. Means ± SE (n = 12 mice/group). $^{\alpha}P < 0.05$ vs. PBS-treated control mice.

progressed over the 60-day postexposure period. A unique finding of the present investigation was the rapid, dose-dependent, and progressive development of interstitial fibrosis in pulmonary regions distant from deposition sites of SWCNT aggregates. This progressive fibrosis occurred in the absence of persistent inflammation. Preliminary data indicate that this interstitial fibrosis is associated with deposition of dispersed SWCNT structures. The mechanism for this interstitial fibrotic response differs from mechanisms proposed for classical fibrogenic particles in that it is not driven by chronic inflammation and chronic activation of alveolar macrophages. Indeed, the interstitial fibrotic response to SWCNT is not mimicked by an equivalent mass exposure to either ultrafine carbon black (a reference nanoparticle) or fine crystalline silica (a classic fibrogenic particle).

Results of this study suggest that if workers are exposed to respirable SWCNT particles at the current PEL (for graphite particles), they may be at risk of developing some lung lesions. The OSHA PEL for graphite is based on an exposure concentration of 5.0 mg/m^3. Human breathing graphite particles with a mass median aerodynamic diameter of 5 μm and ventilatory parameters of 18 bpm with a tidal volume of 500 ml would have a total lung deposition of ~40 mg in 20 work days (8 h/day) of exposure, assuming an airway deposition efficiency of 8.3% and alveolar deposition efficiency of 1.1%. For this work period the alveolar deposition in a worker would be ~4.7 mg. For particles of 5 μm, the majority of this deposition would be in the proximal alveolar region of the lungs, which accounts for ~1/200 of the total lung surface area (58 m^2) or 0.3 m^2 (26). The proximal alveolar dose per unit of alveolar surface area would be 15.7 mg/m^2 for the human lung. As shown in the results, the aspirated SWCNT in the mouse is predominantly deposited in the proximal alveolar region of the lungs. The proximal alveolar region of the mouse is ~0.0006 m^2 (26). Approximately half of the 20-μg dose is deposited in the proximal alveolar region. Thus the proximal alveolar dose per unit of alveolar surface area would be 16.6 mg/m^2, approximately the same as that estimated for a worker exposed to the OSHA PEL for graphite over a period of 20 work days.

We recently investigated potential exposure levels of workers to SWCNT in a small-scale laboratory production facility (17). Although the observed airborne particle concentrations were low (<50 μg/m^3), the amount of material produced was very small (several grams), and significant care was taken to reduce product loss during handling. Agitation of the material by vortexing generated significantly higher levels of respirable SWCNT material. Thus, under large-scale manufacturing conditions, the potential for significant worker exposure may exist. The mice in our study were exposed via a bolus exposure technique, pharyngeal aspiration, which provides widespread delivery of particles throughout the lung but delivers those particles at a single time point (21). Data from nebulization studies suggest that aspiration would generate both SWCNT aggregates and dispersed structures (Fig. 1). However, aspiration of these particles has the same limitations as other bolus exposure techniques, including the nonphysiological rapid delivery of the particles, the possible delivery of nonrespirable aggregates, and the bypassing of the nose (9). However, when particle deposition was comparable, pulmonary responses to bolus instillation tended to reflect the pulmonary response to inhalation (13). It is clear that the rapid fibrogenic response to aspiration of SWCNT argues strongly for a more extensive inhalation study. Efforts are ongoing to develop generation techniques to make such a study feasible.

In conclusion, our results demonstrate that pharyngeal aspiration of SWCNT induces a robust acute inflammatory reaction with the very early onset of a fibrogenic response and the formation of granulomas in C57BL/6 mice. The formation of granulomas is mainly associated with deposition of dense micrometer-scale SWCNT aggregates. However, a unique fibrogenic response is apparent in alveolar septa distant from deposition sites of aggregates and in the absence of persistent inflammation. In addition, pulmonary exposure to SWCNT caused persistent changes in pulmonary functions and decreased bacterial clearance.

GRANTS

This work was supported by National Institute for Occupational Safety and Health Grant 1RO1 OH-008282 and by National Institutes of Health Grant 1RO1 HL-070755.

DISCLOSURES

The findings and conclusions in this report are those of the authors and do not necessarily represent the views of the National Institute for Occupational Safety and Health.

REFERENCES

1. **Adelman P, Baierl T, Drosselmeyer E, Politis C, Polzer G, Seidel A, and Steinleitner C.** Effect of fullerenes on alveolar macrophages in vitro. Institut für Nukleare Festkörperphysik, Karlsruhe, Germany. In: *Toxic and Carcinogenic Effect of Solid Particles in the Respiratory Tract*, edited by Mohr U, Dungworth DL, Mauderly J, Oberdoester G. Washington, DC: ILSI Press, 1994, p. 405–407.
2. **Adler A, Cieslewicz G, and Irvin CG.** Unrestrained plethysmography is an unreliable measure of airway responsiveness in BALB/c and C57BL/6 mice. *J Appl Physiol* 97: 286–292, 2004.
3. **Arepalli S, Nikolaev P, and Gorelik O.** Protocol for the characterization of SWCNT material quality. *Carbon* 42: 1783–1791, 2004.
4. **Arepalli S, Nikolaev P, and Gorelik O.** Analytical characterization of single wall carbon nanotubes. In: *Encyclopedia of Nanoscience and Nanotechnology*, 2004, vol. 1, p. 51–66.
5. **Birch ME.** Elemental carbon monitoring of diesel exhaust particulate in the workplace. In: *NIOSH Manual of Analytical Methods (NMAM 5040)* (4th ed.). Cincinnati, OH: NIOSH, 2003, chapt. Q (DHHS publication no. 2003-154).
6. **Bronikowski MJ, Willis PA, Colbert DT, Smith KA, and Smalley RE.** Gas-phase production of carbon single-walled nanotubes from carbon monoxide via the HiPco process: a parametric study. *J Vac Sci Technol* 19: 1800–1805, 2001.
7. **Cherukur P, Bachilo SM, Litovsky SH, and Weisman RB.** Near-infrared fluorescence microscopy of single-walled carbon nanotubes in phagocytic cells. *J Am Chem Soc* 126: 15638–15639, 2004.
8. **Dresselhaus MS, Dresselhaus G, Charlier JC, and Hernandez E.** Electronic, thermal and mechanical properties of carbon nanotubes. *Philos Transact Ser A Math Phys Eng Sci* 362: 2065–2098, 2004.
9. **Driscoll KE, Costa DL, Hatch G, Henderson R, Oberdorster G, Salem H, and Schlesinger RB.** Intratracheal instillation as an exposure technique for the evaluation of respiratory tract toxicity: uses and limitations. *Toxicol Sci* 55: 24–35, 2000.
10. **Elder AC, Gelein R, Azadniv M, Frampton M, Finkelstein J, and Oberdorster G.** Systemic effects of inhaled ultrafine particles in two compromised, aged rat strains. *Inhal Toxicol* 16: 461–471, 2004.
11. **Ghanem MM, Porter D, Battelli LA, Vallyathan V, Kashon ML, Ma JY, Barger MW, Nath J, Castranova V, and Hubbs AF.** Respirable coal dust particles modify cytochrome P4501A1 (CYP1A1) expression in rat alveolar cells. *Am J Respir Cell Mol Biol* 31: 171–183, 2004.
12. **Gorelik O, Nikolaev P, and Arepalli S.** *Purification Procedures for Single-Walled Carbon Nanotubes. NASA Contractor Report*. Hanover, MD: NASA, 2000 (NASA/CR-2000-208926).
13. **Henderson RF, Driscoll KE, Harkema JR, Lindenschmidt RC, Chang IY, Maples KR, and Barr EB.** A comparison of the inflammatory response of the lung to inhaled versus instilled particles in F344 rats. *Fundam Appl Toxicol* 24: 183–197, 1995.
14. **Huzcko A, Lange H, Calko E, Grubek-Jaworska H, and Droszcz P.** Physiological testing of carbon nanotubes: are they asbestos-like? *Fullerene Sci Technol* 9: 251–254, 1997.
15. **Junqueira LC, Bignolas G, and Brentani RR.** Picrosirius staining plus polarization microscopy, a specific method for collagen detection in tissue sections. *Histochem J* 11: 447–455, 1979.
16. **Lam CW, James JT, McCluskey R, and Hunter RL.** Pulmonary toxicity of carbon nanotubes in mice 7 and 90 days after intratracheal instillation. *Toxicol Sci* 77: 126–134, 2004.
17. **Maynard AD, Baron PA, Foley M, Shvedova AA, Kisin ER, and Castranova V.** Exposure to carbon nanotube material: aerosol release during the handling of unrefined single walled carbon nanotube material. *J Toxicol Environ Health* 67: 87–107, 2004.
18. **NIOSH.** *Pocket Guide to Chemical Hazards-Index of chemical names*. Cincinnati, OH: NIOSH, 2004 (NIOSH publication no. 97-140).
19. **Oberdorster G, Sharp Z, Atudorei V, Elder A, Gelein R, Lunts A, Kreyling W, and Cox C.** Extrapulmonary translocation of ultrafine carbon particles following whole-body inhalation exposure of rats. *J Toxicol Environ Health A* 65: 1531–1543, 2002.
20. **Piguet PF, Collart MA, Grau GE, Sappino AP, and Vassalli P.** Requirement of tumour necrosis factor for development of silica-induced pulmonary fibrosis. *Nature* 344: 245–247, 1990.
21. **Rao GV, Tinkle S, Weissman DN, Antonini JM, Kashon ML, Salmen R, Battelli LA, Willard PA, Hoover MD, and Hubbs AF.** Efficacy of a technique for exposing the mouse lung to particles aspirated from the pharynx. *J Toxicol Environ Health* 66: 1441–1452, 2003.
22. **Roco MC.** Science and technology integration for increased human potential and societal outcomes. *Ann NY Acad Sci* 1013: 1–16, 2004.
23. **Royal Society and Royal Academy of Engineering.** *Nanoscience and Nanotechnologies*. London: Royal Society and Royal Academy of Engineering, 2004 (http://www.nanotec.org.uk/finalReport.htm).
24. **Scott CD, Povitsky A, Dateo C, Gokcen T, Willis PA, and Smalley RE.** Iron catalyst chemistry in modeling a high-pressure carbon monoxide nanotube reactor. *J Nanosci Nanotechnol* 3: 63–73, 2003.
25. **Shvedova AA, Kisin ER, Murray AR, Schwegler-Berry D, Gandelsman VZ, Baron P, Maynard A, Gunther MR, and Castranova V.** Exposure of human bronchial epithelial cells to carbon nanotubes causes oxidative stress and cytotoxicity. In: *Proc Soc Free Rad Research Meeting, European Section, June 26–29, 2003*. Ioannina, Greece: 2004, p. 91–103.
26. **Stone KC, Mercer RR, Freeman BA, Chang LY, and Crapo JD.** Distribution of lung cell numbers and volumes between alveolar and nonalveolar tissue. *Am Rev Respir Dis* 146: 454–456, 1992.
27. **Tao F, Gonzalez-Flecha B,and Kobzik L.** Reactive oxygen species in pulmonary inflammation by ambient particulates. *Free Radic Biol Med* 35: 327–340, 2003.
28. **Underwood EE.** *Quantitative Stereology*. Reading, MA: Addison-Wesley, 1970.
29. **Warheit DB, Laurence BR, Reed KL, Roach DH, Reynolds GA, and Webb TR.** Comparative pulmonary toxicity assessment of single-wall carbon nanotubes in rats. *Toxicol Sci* 77: 117–125, 2004.